CONEM 2022
CONGRESSO NACIONAL DE ENGENHARIA MECÂNICA
TERESINA - PI

ABCM
XI CONGRESSO NACIONAL DE ENGENHARIA MECÂNICA
DE 07 A 11 DE AGOSTO DE 2022, TERESINA-PI, BRASIL

CONEM2022-0029
MICROSTRUCTURAL AND MECHANICAL CHARACTERIZATION OF 5052-H32 ALUMINUM ALLOY

Julia Brescovici Badke, juliabbadke@gmail.com[1]
Tiago dos Santos, tiago.santos@ufsm.br[1]
Kawe Allan De Lima Goulart, kawe.lima@bruning.com.br[2]
Diego Tolotti de Almeida, diegot@bruning.com.br[2]
Cristiano José Scheuer, cristiano.scheuer@ufsm.br[1]
[1] Technology and Mechanics of Materials Group - *Department of Mechanical Engineering*, UFSM, Santa Maria, RS, Brazil.
[2] Bruning Tecnometal Ltd., 98280-000, Panambi, RS, Brazil.

Abstract: *Aluminium alloys (AA) series 5000 are widely employed in engineering applications due characteristics such as high thermal conductivity, high corrosion resistance, good weldability and formability. Specifically, AA5052 is increasingly replacing steels in marine and automotive industries. Currently, these industries seek continuous improvements regarding their productive processes and product quality, avoiding issues closely related to unsuitable production operations planning. Important tools towards the adequate design of manufacturing process and related final product characteristics are the microstructural and mechanical characterization, which allow identifying conditions leading to variations in the material behavior during processing. In an effort to contribute on this matter, this work aims to evaluate the microstructural and mechanical properties of 5052-H32 aluminum alloy. Microstructural characterization is performed using scanning electron microscopy and X-ray diffraction techniques, while mechanical characterization is conducted means of tensile and hardness tests. The obtained results show that the materials microstructure is constituted by Al_3Fe and Al_3Mg_2 intermetallic particles and Al_2O_3 inclusions precipitated in the aluminum matrix. Plasticity increases regarding the rolling orientation from 0° to 45° and decreases from 45° to 90°, while elasticity has an opposite behavior and hardness is not affected by the rolling direction. The mean and planar anisotropy indexes values indicate the suitability of the material by forming processing. Finally, the strength coefficient and strain hardening exponent values indicate that the alloy has lower formability than other Al alloys used in similar applications.*

Keywords: *AA 5052-H32. Microstructural characterization. Mechanical properties.*

1. INTRODUCTION

The reduction of greenhouse gases in the atmosphere is a topic under discussion not only among scientists, but also among politicians, the general public and government officials. Given the imminent need to reduce their emissions, the Kyoto Protocol established goals for developed countries and economies in transition, with the main objective of mitigating the emission of these gases, especially carbon dioxide (CO_2). In this sense, three market flexibility mechanisms were developed to help meet the reduction targets: joint implementation, emissions trading and the Clean Development Mechanism (CDM). Therefore, developed countries had two options to choose: use of flexibilization mechanisms or investment in more efficient technologies (Godoy, 2013).

Given this scenario, investment in studies and research intensified in Europe, the United States of America and other countries. These studies focus mainly on the automobile industry, where regulations have been implemented in the sales and development of new vehicles, considering the reduction in their mass and CO_2 emission levels, thus creating a challenge for engineers. As a result, the requirement to reduce the weight of passenger vehicles has become mandatory in the development of new vehicles (Kulkarni *et al*., 2018).

Replacing steel with aluminum (Al) in certain automobile components, in order to reduce their weight without, however, reducing their performance, is the ideal solution. This is due to the fact that Al density is one third in relation to steel, and its specific strength and stiffness are of the same order of magnitude (Kelkar *et al*., 2001). Specifically, AA class 5052 is increasingly replacing steels in automotive industries. However, the replacement of steel by Al is not economically viable, since the production cost of Al is about five times higher than that of the steel. This high cost is mainly due to the bauxite refining operation, due to damage to the environment caused by toxic gases emitted by waste resulting from primary processing (Lajarin, 2012)

However, in order to meet the goals established by the Kyoto Protocol, the automotive industry promoted the development of new high-strength Al alloys, and the improvement of already established Al alloys, in order to enable the replacement of steel by Al, mainly in stamped components. In order to optimize the processing routes of these "new" materials, numerical simulations using the Finite Element Method (FEM) and experimental validations in bench tests are usually performed, allowing their feasibility and planning. The performance of such simulations and tests contribute to reducing the execution time and costs of manufacturing operations (Andersson, 2005).

However, for the correct performance of experimental tests and numerical simulations, it is necessary to identify the mechanical behavior of these materials during their processing. This is due to microstructural and strength variations that occur during plastic deformation promoted by processing operations, which generate variations in the material behavior. Therefore, the characterization of the magnitude of these variations and knowledge of their effects is essential to improve the accuracy of software and tests used in planning manufacturing operations, especially with regard to the sheet forming processes (Lajarin, 2012). The characterization of the material's behavior is carried out by means of microstructural evaluation, and the determination of the mechanical properties and the conformability parameters of the materials.

In summary, in order to meet the environmental criteria established by the Kyoto Protocol, the desired increase in the efficiency of vehicles by reducing their weight will be achieved by replacing the materials traditionally used in their manufacture by others with a high strength-stiffness/weight. However, to enable the use of such materials, it is necessary to optimize their processing routes, aiming to make them economically and technically viable. Therefore, it is necessary to predict the behavior of these materials during their processing, through their mechanical and microstructural characterization. In this sense, this work this work aims to evaluate the microstructural and mechanical properties of AA 5052-H32 aluminum alloy.

2. MATERIALS AND METHODS

Table 1 shows the chemical composition of the AA 5052 employed in this research, which was indicated by the material supplier. The alloying elements content are within the intervals established by Aluminum Association as can be confirmed by comparing the values informed in the **Table 1**. The AA 5052 plate was supplied in cold-rolled state with a thickness of 2.5 mm. It is important to highlight that the AA 5052 has H32 work hardening, that is, after hardening the material was stabilized to an intermediate strength value between annealed (O) and ¼ hardened (H12).

Table 1. Chemical composition of AA 5052 alloy.

Chemical element	Mg	Si	Fe	Cu	Mn	Cr	Zn	Al
Composition (wt. %)	2.5	0.23	0.32	0.07	0.07	0.3	0.08	Balance
Aluminum Association	2.2 – 2.8	0.25 Max	0.40 Max	0.1 Max	0.1 Max	0.15-0.35	0.1 Max	Balance

Specimens were laser machining from the commercial plate according to the geometry and dimensions indicated in Figure 1*a*, aiming to carry out the tensile tests. The informed geometry and dimensions were adopted in order to meet the ABNT NBR 6673, ASTM E 646 and DIN EN 10 002-1 standards. This was possible, since none of the three standards establish exact dimensions for the specimens, but minimum and maximum values, within which the specimens meet the test requirements. Specimens were machined at angles of 0, 30, 45, 60 and 90° in relation to the rolling direction (Figure 1*b*). Before carrying out the tensile tests, the specimens were submitted to a finishing operation by manual sanding.

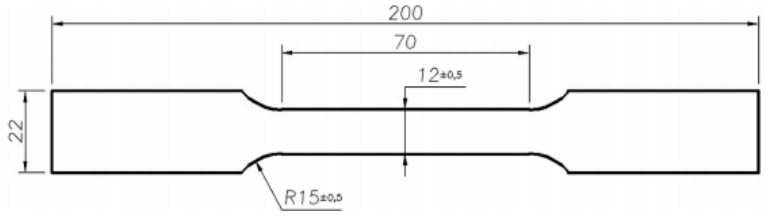

Dimensions given in mm.

(a)

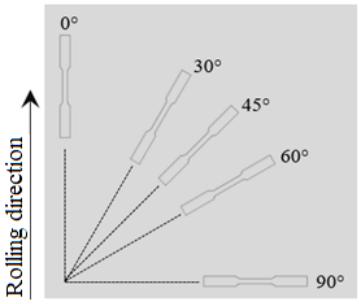

(b)

Figure 1. (a) Specimens shape and dimensions adopted aiming to meet the ABNT NBR 6673, ASTM E 646 and DIN EN 10 002-1 standards for the tensile test execution. (b) Specimens orientation regarding the rolling direction.

The uniaxial tensile tests were carried out in a universal testing machine EMIC® DL100, being executed adopting a standard deformation speed of 0.5 mm/min, in accordance with previously mentioned standards. The programming of the testing machine and obtaining the load and deformation values were performed using the Tesc Emic software installed on a microcomputer interfaced to the universal testing machine. The specimens were uniaxial tensioned until rupture to obtain the engineering tension-deformation curve. With the data of the curve, using the procedures suggested by Garcia *et al.* (2012), were determined the yield (σ_e) and ultimate (σ_u) strength, the Young's modulus (E) and the

percentage elongation (*%Al*). The procedure for determining the strength (*n*) and the strain hardening (*K*) coefficients was performed following the ASTM E-646 standard. To determine the anisotropy indexes, the procedure established by the ASTM E-517 standard was followed. The presented results of the mechanical, conformability and anisotropic properties correspond to the average value of three readings.

The specimens' microstructure and microhardness were also characterized. Using the usual metallographic preparation procedures, samples of untested specimens were prepared through sanding and polishing operations using, in this order, silicon carbide sandpaper of 1200 mesh (due to the used raw material being cold-rolled, it already had a good finish), and metallographic alumina with 1.0 µm size. After preparation, the samples were attacked using Tucker reagent (200 ml of HCl; 200 ml of HNO_3; 200 ml of HF and 200 ml of H_2O), and their microstructure analyzed using an JEOL JSM 6360 scanning electron microscope (SEM). Chemical composition maps were obtained using a BrukerNano Compact energy dispersive X-ray (EDS) spectroscopy system. These same samples were used to perform the Vickers microhardness measurements, which were performed using a Shimadzu HMU-2 microhardness meter. The microhardness measurements were performed using a 300 gf load, with a 15 s load application time. The determination of the phases present was carried out using a Bruker D8 Advance X-ray diffractometer, with CuK radiation (λ = 1.5406 Å), in the Bragg-Brentano (for 2θ angle varying on the 20-110° range) XRD configurations, using scanning speed of 1°/min.

3. RESULTS AND DISCUSSION

Figure 2 shows the SEM micrography and the EDS maps of the sample extracted at 0° regarding the rolling direction. It is verified that undissolved precipitates, distributed in the metallic matrix of aluminum (α-Al), constitute the microstructure of the AA5052-H32 alloy. The SEM micrograph associated with the EDS composition maps allow to infer that the precipitated particles are predominantly Mg and Fe elements. Thus, Fe-based intermetallic probably correspond to the Al_3Fe eutectic component from the Al-Fe system which precipitates due to the Fe content of the alloy (0.32% wt.) exceeds the solubility limit of Fe in the Al matrix. In turn, the Mg-based intermetallic possibly constitute the Al_3Mg_2 phase, which forms after the solubility limit of Mg in the Al matrix is reached (~ 1% wt.), which is much lower than the Mg content of the alloy. It is also possible to identify in the chemical composition maps the presence of oxygen traces, possibly due to the presence of Al_2O_3 inclusions, probably resulting from the bauxite refining operation.

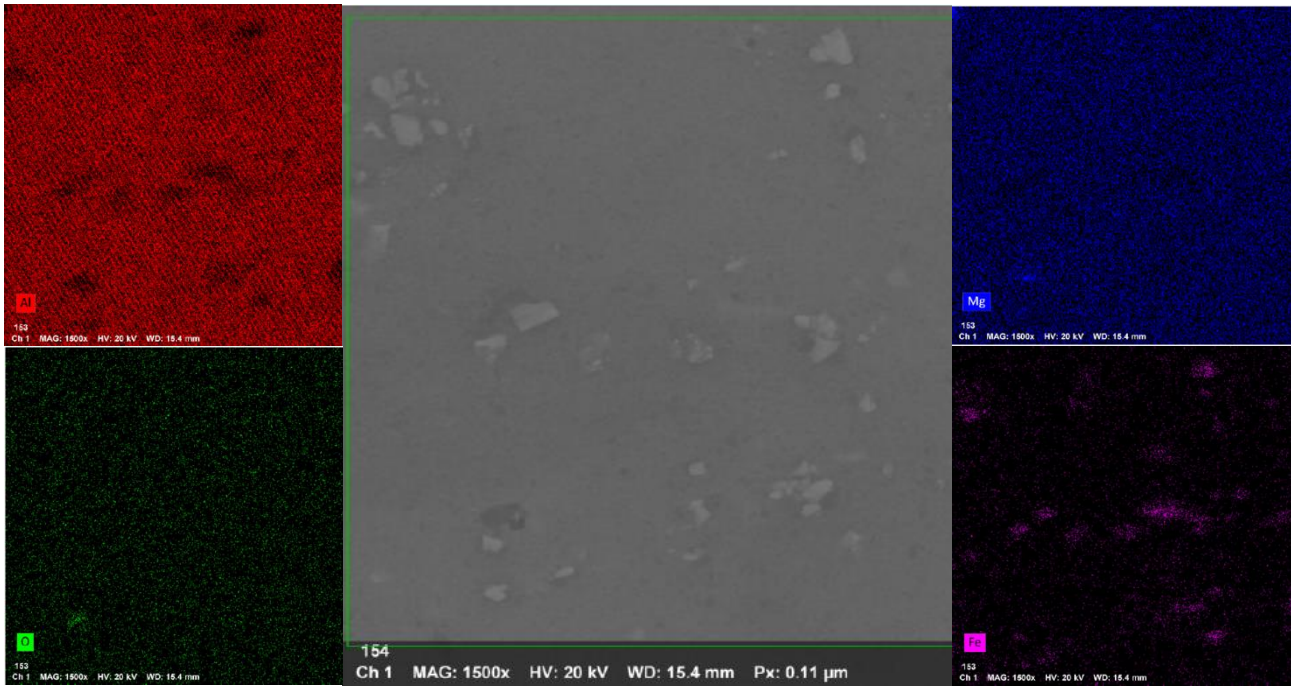

Figure 2. EDS map of the chemical elements distribution from the sample extracted at 0° regarding the rolling direction of the AA5052-H32 alloy.

The X-ray diffraction pattern of AA5052-H32 is shown in Figure 3. According to the reflections identified using the ICDD (International Centre for Diffraction Data) cards, the occurrence of peaks referring to planes of the α-Al phase and Al_3Fe and Al_3Mg_2 precipitates is verified. Regarding the α-Al phase, the diffraction peaks refer to planes (1 1 1), (2 0 0), (2 2 0) and (3 1 1), at diffraction angles of approximately 38°, 45°, 65° and 78°, respectively. In relation to Al_3Fe precipitates, the diffraction peak refers to the (5 3 0) and (4 4 4) plane with diffraction angles of approximately 41.5° and 43°, while the Al_3Mg_2 peak refers to the plane (11 3 3) at a diffraction angles of 39.8°.

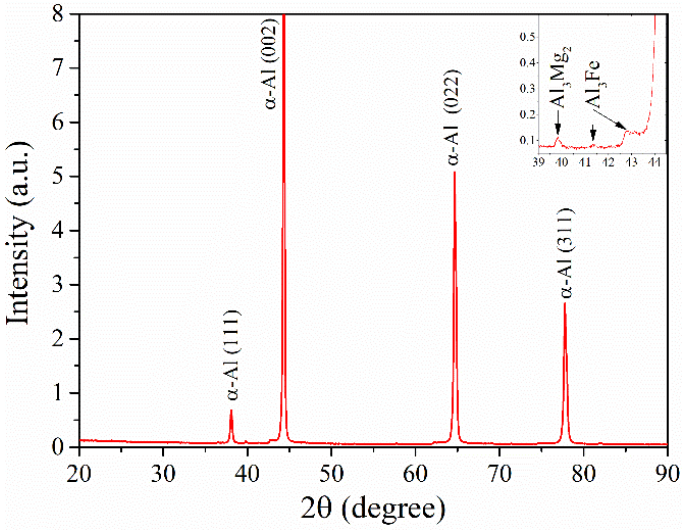

Figure 3. X-ray diffraction pattern of the 5052-H32 specimens.

Figure *4* shows the alloy hardness evolution regarding the rolling direction, measured in the plate plane and cross-section. There is an equality of the measured values both with regard to rolling direction, as well as for the section in which they measured were performed. In the plate plane, the measured values ranged from 64.08 to 71.04 $HV_{0.3}$, while in the cross section the values ranged from 61.18 to 69.31 $HV_{0.3}$. These measured values are similar to those indicated for AA5052-H32 alloy by the Aluminum Association.

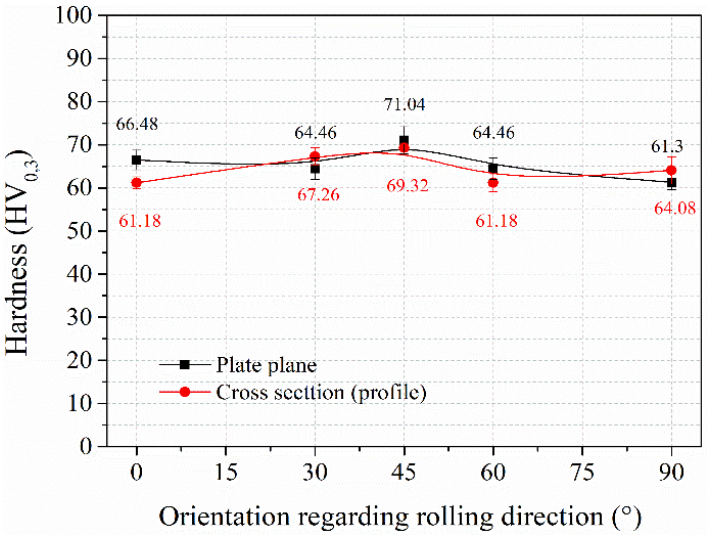

Figure 4. Hardness measured in the plane and cross-section of the samples extracted in different directions regarding the rolling direction of the AA5052-H32 alloy.

In Figure 5 the engineering stress–strain curves are shown. Although slight variations among the curves are observed, in general these variations are small, within the expected variability (15%, according to Garcia *et al.*, 2012). It is worth mentioning the occurrence of a serrated profile, observed in the segment of the engineering stress–strain curves in the uniform work hardening regime. This phenomenon characterizes the occurrence of heterogeneous deformations and is commonly referred to as the Portevin-LeChatelier – PLC effect (Tu *et al.*, 2014; Cottrell, 1953). The PLC effect can be attributed to the effect of intermetallics on the discordance movement during the plastic deformation process that occurred in the uniaxial tensile test (Krishna *et al.*, 2015; Huskins *et al.*, 2010).

The analysis of Figure 5 also allows us to observe that there is no visible change in the profile of the engineering stress–strain curves in the transition among elastic to plastic deformation regimes. For the case of some metals, such as low and medium carbon steels, the elasto-plastic transition is well defined and occurs abruptly, an event called the yield strength limit phenomenon (Callister and Rethwisch, 2012). For the case of aluminum and its alloys, however, the profile of the engineering tension-deformation follows that of the curves in Figure 5, as showed in references Tian *et al.* (2019), Krishna *et al.* (2015), and Huskins *et al.* (2010).

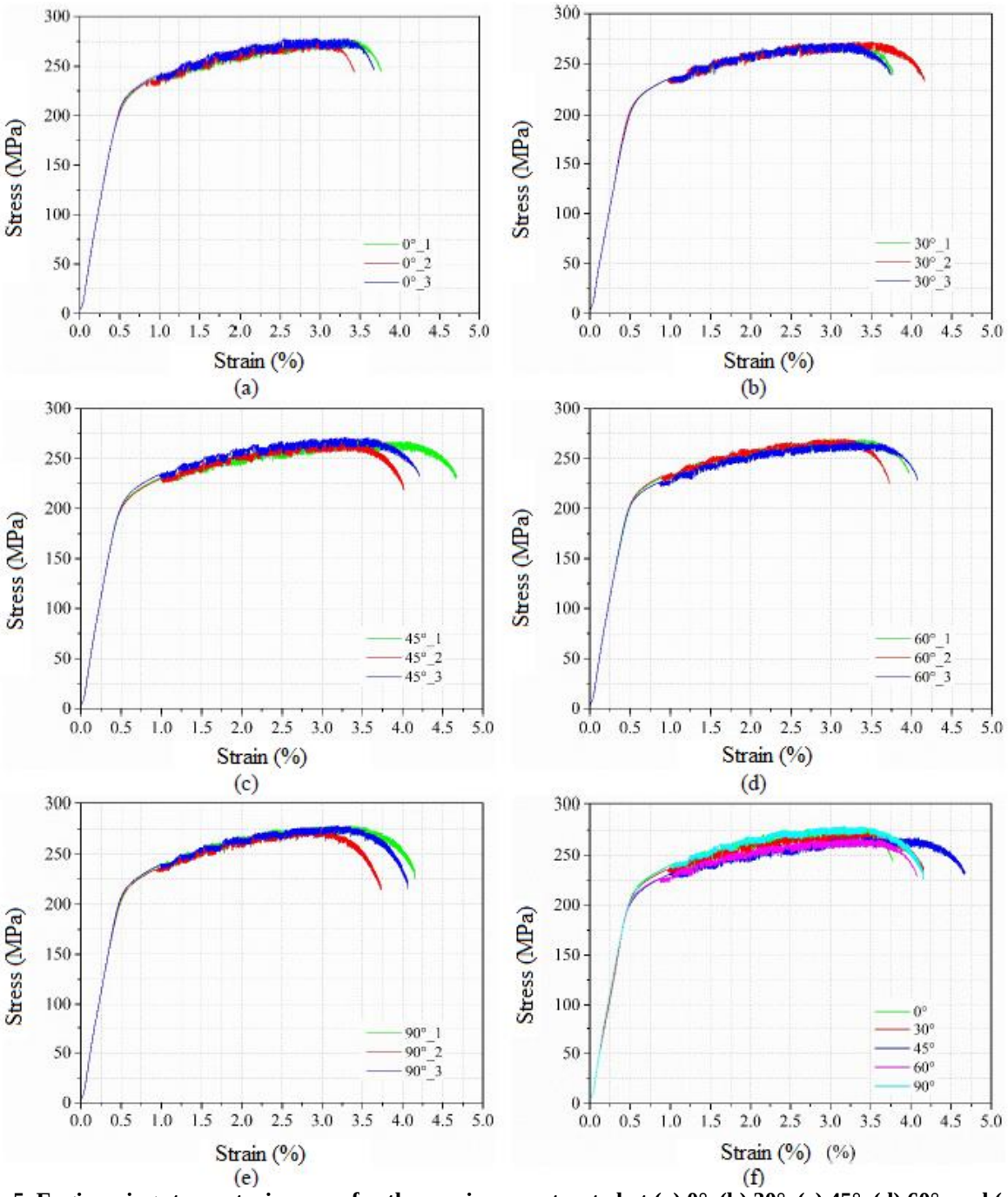

Figure 5. Engineering stress-strain curve for the specimens extracted at (a) 0°, (b) 30°, (c) 45°, (d) 60°, and (e) 90° regarding the rolling direction of the AA5052-H32 alloys. In (f) the comparison between the curves is shown.

It is possible to identify analyzing the comparative curves presented on Figure 5(f), that the stress-strain behavior depends on rolling direction. According to Askeland and Wright (2015), in single crystals the mechanical properties depend on the crystallographic directions. Thus, considering that the mechanical strength of a single crystal is largely anisotropic, an intense plastic deformation that produces a strong preferential orientation will cause a polycrystalline material to have an anisotropy approximately equal to that of a single crystal (DIETER, 1981).

Table 2 shows the anisotropic behavior of yield stress (σ_e) and tensile strength limit (σ_u), Young's modulus (E), and elongation *(%Al)*. It is observed that σ_e and σ_u are smaller in the 45° direction, while *%Al* is larger in this orientation. Similar behavior was reported in the literature by Rioja and Liu (2012) and Liu *et al.* (1998) for pure aluminum and Al-Cu-Li aluminium alloy, respectively; however, this behavior was not justified by the referred authors. To justify such behavior, it should be considered that in the case of specimens oriented at 45° regarding the rolling direction, their grains are aligned at 45° in relation to the direction of load application. Considering that the maximum values of the critical shear stresses in the slip planes are oriented at 45° in relation to the direction of application of the tensile efforts (Bresciani Filho *et al.* 2011), it is expected that these specimens will suffer deformation from lower stress values. It is important to note that the measured σ_e and σ_u values are slightly higher than the values given by the Aluminum

Association for the AA5052-H32 alloy. The mentioned reference indicates a σ_e of 160 MPa, and a σ_u in the range 215 to 265 MPa. The *%Al* value is close to the indicated lower limit (4 to 11%). The measured Young's modulus values are also close to that indicated by Aluminum Association (70 GPa).These small variations among the measured and expected values, may be linked to possible chemical composition variations.

Table 2. Mechanical properties regarding the rolling direction of the AA5052-H32 alloy.

Reference	σ_e (MPa)	σ_u (MPa)	*E* (GPa)	*%Al*
0°	164±4	274±4.3	75,6±3	3.6±0.17
30°	162±4.8	268±5.6	73,6±3	3.8±0.23
45°	155±4.3	265±4.7	73,6±3	4.3±0.33
60°	167±5.2	267±4.9	73,9±3	3.9±0.18
90°	170±6.8	274±4.1	76,4±2	3.9±0.22

Table *3* presents the values of the true deformations in thickness and width (ε_{rb} and ε_{rt}, respectively) and the anisotropy indices calculated from these values. The plastic anisotropy index (r) values for the 0°, 45° and 90° orientations are similar to those reported in the literature (Chaimongkon *et al*., 2019; Barony, 2019; Mohanraj *et al*., 2021). With regard to the normal anisotropy index ($\bar{r}$), the value obtained here (0.847) is of the same order as that obtained by Barony (2019) but higher than that specified by Mohanraj *et al.* (2021) (in this order, 0.885 and 0.626). Regarding the planar anisotropy index (Δr), the value obtained in this work (0.143) is close to that indicated by Mohanraj et al. (2021) and well below the value reported by Barony (2019) (0.131 and 0.213, respectively).

Table 3. Measured plastic anisotropy indexes regarding the rolling direction of the AA5052-H32 alloy.

Reference	ε_{rb}	ε_{rt}	r	$\bar{r}$	Δr
0°	0.0296	0.0570	0.5189	0.8479	|0.1437|
30°	0.0364	0.0478	0.7626		
45°	0.0390	0.0424	0.9198		
60°	0.0408	0.0430	0.9480		
90°	0.0416	0.0403	1.0332		

As indicated by Bresciani Filho *et al.* (2011), the ideal raw materials for deep drawing mechanical forming operations correspond to those that exhibit low values of Δr and high values of $\bar{r}$. This is because high values of $\bar{r}$ suggest that the material will resist to plastic deformation in the thickness direction, maintaining a continuous thickness of the formed product and not showing a tendency to break. On the other hand, low values of Δr suggest that the material will undergo similar deformation in the different directions in which it is deformed, showing no tendency to earing (ripples formed on the edges of components submitted to the deep drawing operation). Based on the indication of Bresciani Filho *et al.* (2011), and considering the values of Δr and $\bar{r}$ calculated here, it can be said that the AA5052-H32 plate characterized here is an appropriate raw material for use in deep drawing operations.

The determined *K* and *n* values are compiled in Table 4 together with the values reliability degree (R^2). According to Dieter (1990), *n* varies from 0 to 1, with the lower limit characterizing a perfectly plastic solid and the upper limit a perfectly elastic solid. According to the cited author, metals generally exhibit *n* values in the range between 0.1 and 0.5. The values of *K*, in turn, depend on the manufacturing operations (thermal, mechanical, chemical treatments and their combinations) to which the material was exposed. According to Rodrigues and Martins (2010), the values of *K* and *n* for commercial purity aluminum correspond to 140 MPa and 0.25. For the AA 5052-H32, alloy, the values of *K* and *n* reported in the literature differ among authors. Mohanraj *et al.* (2021) obtained *K* and *n* mean values of 327.63 and 0.143. Chaimongkon *et al.* (2019), in turn, presented the *K* and *n* values as a function of the alloy rolling orientation, obtaining *K* of 343.58, 336.85 and 348.50 for the angles of 0°, 45° and 90 °; and the *n*, in this order, of 0.1098, 0.1053 and 0.1010. Based on this information, it can be stated that the values found here are in agreement with those reported in the literature.

Table 4. Strength (*n*) and strain hardening (*K*) coefficients values regarding the rolling direction of the AA5052-H32 alloy.

Reference	*n*	R^2	*K* (MPa)
0°	0.1127±0.009	0.9991	328.5±2.27
30°	0.119±0.008	0.9986	328.91±2.646
45°	0.1097±0.019	0.9955	327.48±0.631
60°	0.1137±0.003	0.9992	328.09±2.018
90°	0.132±0,002	0.9994	334.23±2.479

Considering that *K* represents the resistance that the material performs against its deformation, the lower its value, the greater its formability. Therefore, low *K* values are ideal for materials used in mechanical forming operations. The exponent *n*, in turn, quantifies the material's capacity to distribute the deformation along its volume. Thus, materials with high n values are more suitable for application in mechanical forming, as they suffer evenly hardening, reducing the probability of fracture occurring during the operation. According to Garcia *et al.* (2012), low values of n characterize large strain variations promoted by relatively small variations of the stress, in the plastic zone. Thus, such materials tend to restrict work hardening to small volume portions, causing low levels of deformation to bring the material to conditions closer to fracture. Based on this, in view of other alloys commonly used in the automotive industry, such as AA3104-H34 (Kapp, 2021), AA6016, AA6005A, AA6063 and AA6013 (Prillhofer *et al.*, 2014), it can be stated that from the point of view of the formability parameters, there are large variations between these materials, and comparatively alloy 5052-H32 is not the best option.

Substituting the values of the *K* and *n* indexes in the Hollomon equation, obtain the equations that describe the real plastic behavior of the AA5052-H32 as a function of its rolling orientation (Table 5). With the equations reported in Table 5, it is possible to approximate the stress-strain behavior of the AA5052-H32 alloy if the striction was corrected and the work hardening kept uniform.

Table 5. Hollomon equations to describe the plastic behavior of class AA5052-H32 regarding its rolling direction.

Condição	**0°**	**30°**	**45°**	**60°**	**90°**
$\sigma_v : K \cdot \varepsilon^n$	$\sigma_v : 328{,}5 \cdot \varepsilon^{0.1127}$	$\sigma_v : 328.91 \cdot \varepsilon^{0.119}$	$\sigma_v : 327.48 \cdot \varepsilon^{0.1097}$	$\sigma_v : 328.09 \cdot \varepsilon^{0.1137}$	$\sigma_v : 334.23 \cdot \varepsilon^{0.132}$

As expected, Figure 6 shows, for all conditions evaluated, the continuous increase in stress, caused by work hardening, with the increase in strain. Although the curves are similar to each other, it is possible to identify in the detail of the figure a narrow disharmony between the curves obtained for each orientation. It is observed that the curves referring to the 45° and 90° orientations were those that exhibited, in this order, the lowest and highest stress values. This behavior results directly from the values of K obtained for each of these conditions.

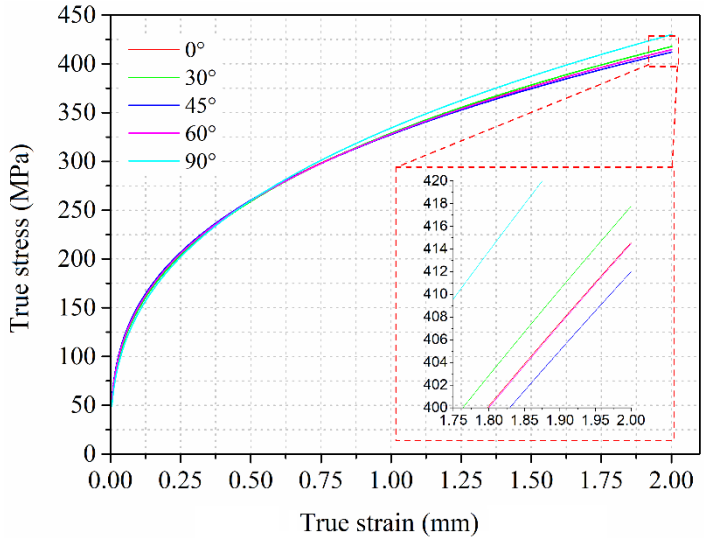

Figure 6. True stress–strain curves of AA 5052-H32 alloy.

4. CONCLUSIONS

From the analysis and discussion of the presented results, it is possible to list the following conclusions:

- The AA5052-H32 alloy microstructure is constituted by intermetallic particles such as Al_3Fe and Al_3Mg_2, and by inclusions of Al_2O_3 in an aluminum matrix (α-Al);
- The hardness values measured as a function of the rolling direction in the plate plane and cross-section are statistically equal;
- The yield stress and tensile strength values decrease from 0° to 45°, and increase from 45° to 90° in relation to the rolling direction;
- Plasticity increases in the range from 0° to 45° in relation to the rolling direction, and decreases from 45° to 90°; while elasticity has the opposite behavior;
- The high value of the medium anisotropy index and the low of the planar anisotropy index indicate the AA5052-H32 alloy suitability for processing by mechanical forming;
- The values of strength and strain hardening coefficients indicate that the alloy has lower formability than other Al alloys used in the automotive sector; and,

- True stress-strain curves indicates a slightly greater resistance to deformation in the 90° orientation relative to the rolling direction.

5. ACKNOWLEDGEMENTS

The authors are grateful to Bruning Tecnometal Ltd. for providing the AA 5052-H32 and specimens machining.

6. REFERENCES

Andersson, A., 2005. Numerical and experimental evaluation of springback in a front side member. **Journal of Materials Processing Technology**, Vol. 169, p. 352-356.

Askeland, D.R.; Wright, W.J. *Ciência e Engenharia dos Materiais*. 2ª ed. São Paulo: Cegage Learnig, 2015

Barony, N.B. *Avaliação estrutural e mecânica de chapas das ligas de alumínio AA 5052 e AA 5050C***.** *(in Portuguese)*. Master Dissertation, Graduate Program in Materials Science, Instituto Militar de Engenharia, Rio de Janeiro, 2019.

Bresciani Filho, E., Silva, I. B., Batalha, G. F., Button, S. T. *Conformação Plástica dos Metais***.** 1ª. ed. São Paulo: EPUSP, 2011.

Coutinho, T.A., 1980. *Metalografia* de *não-ferrosos:* análise e prática *(in Portuguese)*. Editora Blücher, São Paulo.

Cottrell, A., 1953. LXXXVI: A note on the Portevin-Le Chatelier effect. The London, Edinburgh, and Dublin Philosophical Magazine and Journal of Science, Vol. 44, p. 829–832.

Callister, W.D., Rethwisch, D.G., 2012. *Ciência e engenharia de materiais: uma introdução (in Portuguese)*. 8th ed. Editora LTC, São Paulo.

Chaimongkon, T., Uthaisangsuk, V., Panich, S. Anisotropic Fracture Forming Limit Curves of Aluminum Alloy AA5052-H32 Sheet. The Second Materials Research Society of Thailand International Conference AIP Conf. Proc. 2279, 050003-1–050003-8, 2019.

Dieter, G.E., 1981. *Metalurgia Mecânica (in Portuguese)*. 2th ed. Ed. Guanabara Dois, Rio de Janeiro.

Garcia, A.; Spim, J. A.; Santos, C. A. *Ensaio dos Materiais*. 2. ed. Rio de Janeiro: LTC, 2012.

Godoy, S.G.M., 2013. "*Projetos de redução de emissões de gases de efeito estufa: desempenho e custos de transação".* **Revista de Administração**, V. 48, p. 310-326.

Huskins, E., Cao, B., Ramesh, K., 2010. Strengthening mechanisms in an Al–Mg alloy. Materials Science Engineering A, Vol. 527, p. 1292–1298.

Kapp, R.Z. Caracterização Experimental Da Anisotropia Em Chapas De Alumínio Da Série 3XXX classe 3104-H34. Trabalho de Conclusão de Curso (Graduação em Engenharia Mecânica) – Universidade Federal de Santa Maria, Santa Maria, 2021

Kelkar, A., Roth, R., Clark, J., 2001. Automobile Bodeis: Can Alumnum Be an Economical Alternative to Steel? **Automotive Materials Economics**, Vol. 1, p. 27-32.

Krishna, K., Sekhar, K.C., Tejas, R., Krishna, N.N., Sivaprasad, K., Narayanasamy, R., Venkateswarlu, K., 2015. Effect of cryorolling on the mechanical properties of AA5083 alloy and the Portevin–Le Chatelier phenomenon. Materials Design, Vol. 67, p. 107–117.

Kulkarni, S., Edwards D.J., Parn E.A., Chapman C., Aigbavboa C.O., Cornish R., 2018. Evaluation of vehicle lightweighting to reduce greenhouse gas emissions with focus on magnesium substitution. **Journal of Engineering, Design and Technology**, Vol. 16, p. 869-888.

Lajarin, S.F., 2012. *Influência da variação do módulo de elasticidade na previsão computacional do retorno elástico em aços de alta resistência (in Portuguese)*. Doctoral Dissertation, Graduate Program in Mechanical Engineering, Federal University of Parana, Curitiba, Brazil.

Liu, Q., Juul, J.D., Hansen N., 1998. Effect of grain orientation on deformation structure in cold-rolled polycrystalline aluminium. **Acta Materialia**, Vol. 46, p. 5819-5838.

Mohanraj, M., Muhammad, S., Dong, W.J., 2021. Experimental and Numerical Investigation of AA5052-H32 Al Alloy with U-Profile in Cold Roll Forming. **Materials**, Vol. 14, p. 470.

Martins, A.L.T., 2014. *Estudo comparativo de propriedades mecânicas e textura de laminados da liga de alumínio 3104-H19 (in Portuguese)*. Master's Thesis. Graduate Program in Materials, Mackenzie Presbiterian University, São Paulo.

Mugendiran, V., Gnanavel, A., Ramadoss, R., 2014. Tensile Behaviour of Al5052 Alloy Sheets Annealed at Different Temperatures. Advanced Materials Research, Vol. 845, p 431-435.

Prillhofer, R., Rank, G., Berneder, J., Antrekowitsch, H., Uggowitzer, P.J., Pogatscher, S., 2014. Property Criteria for Automotive Al-Mg-Si Sheet Alloys. **Materials,** Vol. 7, p. 5047-5068.

Rioja, R.J., Liu, J., 2012. The Evolution of Al-Li Base Products for Aerospace and Space Applications. **Metallurgical and Materials Transactions A**, Vol. 43, p. 3325–3337.

Rodrigues, J., Martins, P. *Tecnologia Mecânica: Tecnologia da Deformação Plástica. Vol. I – Fundamentos teóricos* 2ª. ed. Lisboa: Escolar Editora, 2010.

Souza, S.A., 1982. *Ensaios de Materiais Metálicos (in Portuguese)*. 5th. Editora Blucher, São Paulo.

Tian, N., Yuan, F., Duan, C., Liu, K., Wang, G., Zhao, G., Zuo, L., 2019. Prediction of the Work-Hardening Exponent for 3104 Aluminum Sheets with Different Grain Sizes. Materials, Vol. 12, p. 2368.

Tu, Y.Y., Qian, H., Zhou, X.F., Jiang, J.Q., 2014. Effect of Scandium on the Interaction of Concurrent Precipitation and Recrystallization in Commercial AA3003 Aluminum Alloy. Journal of Metallurgical and Materials Transactions. A Vol. 45, p 1883–1891.

7. RESPONSIBILITY NOTICE

The authors are the only responsible for the printed material included in this paper.